IL NUOVO CIMENTO **48 C** (2025) 88
DOI 10.1393/ncc/i2025-25088-y

Colloquia: IFAE 2024

First evidence of $B \to K\nu\overline{\nu}$ and recent results on radiative decays at Belle and Belle II(*)

G. Gaudino(1)(2)

(1) *Scuola Superiore Meridionale - Napoli, Italy*
(2) *INFN Sezione di Napoli - Napoli, Italy*

received 2 December 2024

Summary. — This proceeding summarized recent measurement of the Radiative decay of the B meson, with also a more detailed section on the first evidence of the $B^+ \to K^+\nu\overline{\nu}$ at Belle II.

1. – Introduction

In the Standard Model (SM), transitions involving Flavour Changing Neutral Currents (FCNC) are forbidden at the tree level, and occur through electroweak loop diagrams. Beyond-the-SM (BSM) physics can either contribute to the loop diagrams or directly appear at tree level, altering various physics observables from their SM predictions. A typical FCNC transition is the radiative decay of a B meson to the inclusive final state $X_s\gamma$, where X_s includes all the possible mesons with a strange quark. This decay offers excellent sensitivity to BSM effects. The photon-energy spectra can also provide insights into SM parameters.

A similar transition with the same characteristics, and a similar Feynman diagram is the $b \to s\ell\ell$, in particular $b \to s\nu\overline{\nu}$.

Belle II provided different measurement of these kinds of transitions, in particular, Belle II provided the first evidence of the $B^+ \to K^+\nu\nu$ channel.

2. – The Belle II detector, experimental data and MC simulations

The Belle II experiment, situated at the SuperKEKB collider in Tsukuba, Japan, primarily collected data at the $\Upsilon(4S)$ resonance, focusing on B meson decays. Key components of the Belle II detector include the Vertex Detector, which is composed of Pixel Detector (PXD) and a Silicon Vertex Detector (SVD) for micrometric-level vertexing and tracking below 50 MeV of transverse momentum, the Central Drift Chamber (CDC) for momentum measurements, Time-Of-Propagation (TOP) counters and ring-imaging Cherenkov counters for particle identification (ARICH), an Electromagnetic Calorimeter (ECL) for detecting electrons, photons and neutral particles, and an RPC system (KLM) for muon and K_L detection.

(*) IFAE 2024 - "Intensity Frontier" session

The dataset used for analysis in this report comprises an integrated luminosity of 189 fb^{-1} (from 2019 to 2021). Experimental results are interpreted and compared with Standard Model predictions using Monte Carlo simulations, employing software packages such as EvtGen [2], Pythia [1], and kkmc [3]. The full detector responses and simulations are executed with Geant4, while data and Monte Carlo reconstructions are performed using the Belle II analysis software framework, `basf2` [4].

Full Event Interpretation: `FEI`. – The Full Event Interpretation (FEI) [5] is an algorithm used in the Belle II experiment to categorize events into signal-side (the B decay) and tag-side (the other B produced in the event). It provides crucial details about B-decays, such as event type (*e.g.*, $q\bar{q}$, $\tau\tau$ or $B\overline{B}$, decay vertex, and the reconstructed four-momentum of tag and signal B mesons. FEI employs Multivariate Classifiers for each decay channel and is trained on Monte Carlo data within the `basf2` software package. The method, used with a hadronic tagging approach, offers high purity but limited tagging efficiency compared to semileptonic tagging, where hadronic tag means a $B_{\rm tag}$ decay in only hadronic particles and semileptonic means a $B_{\rm tag}$ decay with at least one lepton in the final state. In all the analyses presented here, the hadronic tagging method is employed.

3. – Search for $B^+ \to K^+\nu\bar{\nu}$ decay

The Standard Model (SM) predicts the branching fraction of the $B^+ \to K^+\nu\bar{\nu}$ decay to be $\mathcal{B}(B^+ \to K^+\nu\bar{\nu}) = (5.58 \pm 0.37) \times 10^{-6}$ [6]. However, models that incorporate non-SM particles could significantly alter this prediction. To date, all analyses have found no evidence of a signal, with the current experimental upper limit on the branching fraction is set at 1.6×10^{-5} at the 90% confidence level [7].

Belle II conducted a measurement [8] using the full Run 1 dataset, employing both Inclusive Tagging Analysis (ITA) and Hadronic Tagging Analysis (HTA) methods. The ITA method, known for its sensitivity, and the more conventional HTA method were employed with nearly independent samples.

Details of the ITA method, crucial for achieving high precision, and the combined results of ITA and HTA will be discussed. An identification of the signal kaon candidate was required, with selection based on the smallest mass squared of the neutrino pair, defined as $q^2_{\rm rec} = s/(4c^4) + M_K^2 - \sqrt{sE_K^*/c^4}$, assuming the signal B meson is at rest in the e^+e^- center-of-mass frame. Here, M_K denotes the known mass of K^+ meson, and E_K^* represents the reconstructed energy of the kaon in the center-of-mass system. Background suppression employed event shape, kinematics, vertexing, and missing energy information via two Boosted Decision Trees (BDT1 and BDT2). A sample-composition fit in bins of the BDT2 output (η(BDT2)) and $q^2_{\rm rec}$ was used to extract the signal branching fraction relative to the SM prediction (signal strength μ). Various control samples validated the background modeling in simulated events, with correction factors and systematic uncertainties derived as needed. The main sources of systematics are related to background which can mimic the signal and also the knowledge of the branching ratios, which are used to build the Monte Carlo templates. Several systematic uncertainties were considered, including normalization of $B\bar{B}$ backgrounds, limitations of simulated sample sizes, and modeling of $B^+ \to K^+K_LK_L$ and $B \to D^{**}\ell\nu$ decays. Figure 1 shows the data in the signal regions for both ITA and HTA, overlaid with fit results.

As a validation of the ITA approach, the branching fraction for $B^+ \to \pi^+K^0$ decay was measured with minimal adaptation of the ITA strategy, yielding results consistent with the world average.

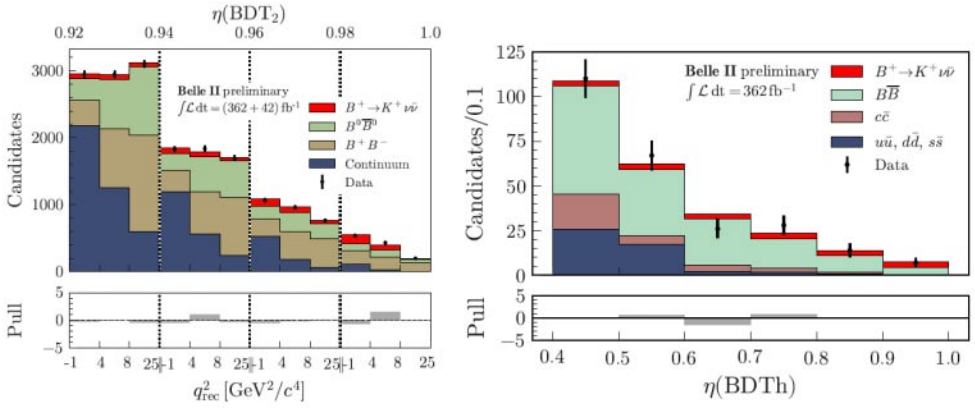

Fig. 1. – Observed yield and fit result of $\eta(BDT2) \times q^2$ and of η(BDTh) as obtained by the ITA (left) and the HTA (right) fits. The pull distribution are shown in the bottom panel.

For HTA, signal extraction relied on the classifier output (η(BDTh)) used in background suppression. Good agreement between data and fit was observed in both samples. ITA yielded a signal strength of $\mu = 5.4 \pm 1.0(\text{stat}) \pm 1.1(\text{syst})$, corresponding to a 3.5σ excess over the background-only hypothesis and a 2.9σ deviation from the SM expectation. HTA results showed $\mu = 2.2^{+1.8}_{-1.7}(\text{stat})^{+1.6}_{-1.1}(\text{syst})$, corresponding to a 1.1σ excess over the background-only hypothesis and a 0.6σ deviation from the SM expectation. ITA and HTA results agreed at the 1.2σ level. The combined signal strength yielded $\mu = 4.6 \pm 1.0(\text{stat}) \pm 0.9(\text{syst})$, corresponding to a branching fraction for $B^+ \to K^+\nu\bar{\nu}$ decay of $[2.3 \pm 0.5(\text{stat})^{+0.5}_{-0.4}(\text{syst})] \times 10^{-5}$. The significance with respect to the background-only hypothesis was 3.5 standard deviations, marking the first evidence for $B^+ \to K^+\nu\bar{\nu}$ decay. The combined result was 2.7 standard deviations above the SM expectation. Compared to previous measurements [8], the ITA result agreed with previous hadronic-tag and inclusive measurements, though it exhibited a 2σ tension with measurements using semileptonic B tag. The HTA result agreed with all previous measurements and represented the most precise result using the hadronic tag method to date.

4. – Search for New Physics in Radiative B Decays

This section summarizes two radiative measurements performed at Belle and Belle II (full Run 1 dataset):

1) $B \to \gamma\gamma$: this analysis is conducted using data from both Belle and Belle II.

2) $B \to K^*\gamma$: this analysis utilizes data solely from Belle II.

Both analyses involve a full reconstruction of the B decay. The key discriminative variables are the beam-constrained mass, $M_{bc} = \sqrt{s/4 - p^{*2}_B}$, and the energy difference with the beam energy, $\Delta E = E^*_B - \sqrt{s}/2$. The main backgrounds for radiative B decay analysis arises from asymmetric π^0/η decays and continuum $e^+e^- \to q\bar{q}$ events.

TABLE I. – *Summary of $\mathcal{BR}(B^0 \to \gamma\gamma)$ measurements and upper limits (UL) at 90% confidence level.*

	$\mathcal{BR}(B^0 \to \gamma\gamma) \times 10^8$	UL on $\mathcal{BR}(B^0 \to \gamma\gamma) \times 10^8$
Belle	$(5.4^{+3.3}_{-2.6} \pm 0.5)$	< 9.9
Belle II	$(1.7^{+3.7}_{-2.4} \pm 0.3)$	< 7.4
Combined	$(3.7^{+2.2}_{-1.8} \pm 0.5)$	< 6.4

To mitigate these backgrounds, most radiative B decay analyses employ multivariate discriminators, which are trained using Monte Carlo samples.

In the $B \to \gamma\gamma$ analysis, the final fit is performed using the three variables described above: M_{bc}, ΔE, and C_{BDT}, the output of the background suppression Boosted Decision Tree. The final result of this analysis is the branching ratio of the $B \to \gamma\gamma$ decay. The Belle, Belle II, and combined results are reported in table I.

In the $B \to K^*\gamma$ analysis, the final fit is performed using only M_{bc} and ΔE. The final results include the branching ratio, the $\mathcal{CP}$ asymmetries $\mathcal{A}_{CP}(\%)$, and the differences $\Delta\mathcal{A}_{CP}$. The $\mathcal{A}_{CP}$ is defined as:

$$\mathcal{A}_{CP} = \frac{N_{\bar{B}}/\varepsilon_{\bar{B}} - N_B/\varepsilon_B}{N_{\bar{B}}/\varepsilon_{\bar{B}} + N_B/\varepsilon_B} \tag{1}$$

where ε represents the selection efficiency for a given $B \to K^*\gamma$ channel for the B (or $\bar{B}$) sample, which includes the $\pi^0 \to \gamma\gamma$ and $K_S \to \pi^-\pi^+$ branching fractions where applicable. The results of different physics observables are listed in table II.

TABLE II. – *Measured branching fractions, $\mathcal{A}_{CP}(\%)$, $\Delta\mathcal{A}_{CP}(\%)$, and Δ_{0+} for $B \to K^*\gamma$ channels. The first quoted uncertainties are statistical, and the second are systematic.*

Channel	$\mathcal{A}_{CP}(\%)$	$\mathcal{BR}(\%)$
$B^0 \to K^{*0}[K^+\pi^-]\gamma$	$(-3.2 \pm 2.4 \pm 0.4)$	$(4.15 \pm 0.10 \pm 0.11)$
$B^0 \to K^{*0}[K_S\pi^0]\gamma$	-	$(4.24 \pm 0.37 \pm 0.23)$
$B^0 \to K^{*0}\gamma$	$(-3.2 \pm 2.4 \pm 0.4)$	$(4.16 \pm 0.10 \pm 0.11)$
$B^+ \to K^{*+}[K^+\pi^0]\gamma$	$(1.5 \pm 4.2 \pm 0.9)$	$(3.91 \pm 0.18 \pm 0.19)$
$B^+ \to K^{*+}[K_S\pi^+]\gamma$	$(-3.5 \pm 4.3 \pm 0.7)$	$(4.13 \pm 0.19 \pm 0.13)$
$B^+ \to K^{*+}\gamma$	$(-1.0 \pm 3.0 \pm 0.6)$	$(4.04 \pm 0.13 \pm 0.13)$
$B \to K^*\gamma$	$(-2.3 \pm 1.9 \pm 0.3)$	$(4.12 \pm 0.08 \pm 0.11)$
	$\Delta\mathcal{A}_{CP}(\%)$	$\Delta_{0+}(\%)$
$B \to K^*\gamma$	$(2.2 \pm 3.8 \pm 0.7)$	$(5.1 \pm 2.0 \pm 1.5)$

REFERENCES

[1] Sjöstrand T. *et al.*, *Comput. Phys. Commun.*, **191** (2015) 159, arXiv:1410.3012 [hep-ph].
[2] Lange D. J., *Nucl. Instrum. Methods Phys. Res. A*, **462** (2001) 152.
[3] Jadach S., Ward B. F. L. and Was Z., *Comput. Phys. Commun.*, **130** (2000) 260, arXiv:hep-ph/9912214.
[4] Belle-II Framework Software Group (Kuhr T. *et al.*), *Comput. Softw. Big Sci.*, **3** (2019) 1, arXiv:1809.04299 [physics.comp-ph].
[5] Keck T., Abudinén F., Bernlochner F. U., Cheaib R., Cunliffe S., Feindt M., Ferber T., Gelb M., Gemmler J., Goldenzweig P. *et al.*, *Comput. Softw. Big Sci.*, **3** (2019) 6, arXiv:1807.08680 [hep-ex].
[6] Parrott W. G., Bouchard C. and Davies C. T. H., *Phys. Rev. D*, **107** (2023) 014511.
[7] Particle Data Group *et al.*, *Prog. Theor. Exp. Phys.*, **2022** (2022) 083C01.
[8] Belle II Collaboration (Adachi I. *et al.*), *Phys. Rev. D*, **109** (2024) 112006.